ELECTRON CLOUD EFFECTS IN SUPERKEKB COMMISSIONING

K. Ohmi *, J. Flanagan, H. Fukuma, H. Ikeda, E. Mulyani, K. Shibata, Y. Suetsugu, M. Tobiyama,
KEK, Tsukuba, Japan, also at Soken-dai, Tsukuba, Japan

Abstract

A vertical emittance growth (beam size blow-up) due to electron cloud has been observed in the positron low energy ring (LER) in Phase-I commissioning (2016) of SuperKEKB. The emittance growth is caused by fast head-tail instability due to wake force induced by electron cloud. The emittance growth was suppressed by weak permanent magnets generating longitudinal field, which cover the drift space of the ring in Phase-II (2018). The emittance growth has been studied during the commissioning with measuring electron cloud density in the beam chamber. We discuss threshold of the electron density for the instability.

INTRODUCTION

The electron cloud instabilities, vertical fast head-tail instability [1] and fast coupled bunch instability [2], were key issues in KEKB. The instabilities have also been regarded as a problem in SuperKEKB. In SuperKEKB, cure of electron cloud was one of the highest priority issue. A target electron cloud density to manage the instability has been evaluated theoretically and numerically, and the vacuum system has been designed to realize the target density. Antechambers with TiN coating and grooved surface were adopted in arc section. TiN coating was applied also in straight section chambers [3].

Beam commissioning of Phase-I was performed in February to June in 2016 without interaction region and Phase-II commissioning was performed in March to July 2018 after installation of IR magnets and the BELLE-II detector. Study of electron cloud effects in the positron ring (LER) was important subject in the commissioning. Vertical emittance growth due to electron cloud has been observed in the positron ring (LER) in Phase-I commissioning. The emittance growth was suppressed by weak permanent magnets, which cover the drift space of the ring in Phase-II commissioning. Electron cloud density has been monitored during the commissioning and the threshold for the electron cloud instability has been studied in various operating beam conditions. Electron cloud has been monitored at an aluminium test chamber w and w/o TiN coating. Table 1 summarizes parameters of SuperKEKB LER. Bunches were filled by 3 bucket (6 ns spacing) in the commissioning, while they are filled by 2 bucket (4ns spacing) in the design. Maximum operating current 1 A was achieved at the total number of bunches 1576, to be compared with 3.6 A for 2500 bunches in the design.

* ohmi@post.kek.jp

Table 1: Parameter list of SuperKEKB LER

	Phase I, II	Design
Circumference, L (m)	3016.3	
Energy, E (GeV)	4	
Current, I (A)	1	3.6
Number of bunch, N_b	1576	2500
Bunch population, N_p (10^{10})	≤ 5	9
Emittance, $\varepsilon_{x/y}$ (nm/pm)	2.1/15	3.2/9
Bunch length, σ_z (mm)	6	
Synchrotron tune, ν_s	0.02	0.022

PREDICTION FOR ELECTRON CLOUD INSTABILITIES IN SUPERKEKB

Threshold of electron density was evaluated by a simulation code PEHTS. Electron cloud is generated at 16 points in the LER ring. Beam motion is integrated over 16 steps per revolution interacting with electron cloud. Figure 1 presents simulation results for single bunch instability caused by electron cloud. Top plot shows evolution of vertical beam size for various electron density. The threshold density is estimated as $\rho_{e,th} = 3.8 \times 10^{11}$ m^{-3} at the design parameters of SuperKEKB. Bottom plot shows vertical position ($y_e(t = z/c)$) of electron cloud during interaction with a bunch and vertical position ($y(z)$) and size ($\sigma_y(z)$) of the bunch at 400-th turn for the density $\rho_e = 4.2 \times 10^{11}$ m^{-3}. Clear signal of head-tail instability and collective motion of electron cloud are seen. This head-tail motion appears as vertical emittance growth of positron beam.

The single bunch instability is caused by a vertical wake force induced by electron cloud. The wake force is expressed by [4].

$$W(z) = c\frac{R_S}{Q} e^{\omega_c z/(2cQ)} \sin\frac{\omega_c z}{c} \tag{1}$$

where

$$c\frac{R_S}{Q} = K\frac{2\sqrt{2}\pi^{3/2}\rho_e L}{N_p}\frac{\omega_c\sigma_z}{c}. \tag{2}$$

ω_c is coherent frequency of vertical motion of electron cloud with the same transverse size as beam ($\sigma_x \times \sigma_y$),

$$\omega_c^2 = \frac{N_p r_e c^2}{\sqrt{2\pi}\sigma_z\sigma_x\sigma_y} \tag{3}$$

where the positron beam is flat, $\sigma_x \gg \sigma_y$. A small frequency shift $\omega_c\sqrt{1 - 1/(4Q^2)} \approx \omega_c$ is neglected. Incoherent frequency for an electron is $\omega_e = \sqrt{2}\omega_c$.

Two particle model is available for $\omega_c\sigma_z/c \sim 1$. Coasting beam model is desirable for $\omega_c\sigma_z/c > 1$. The stability

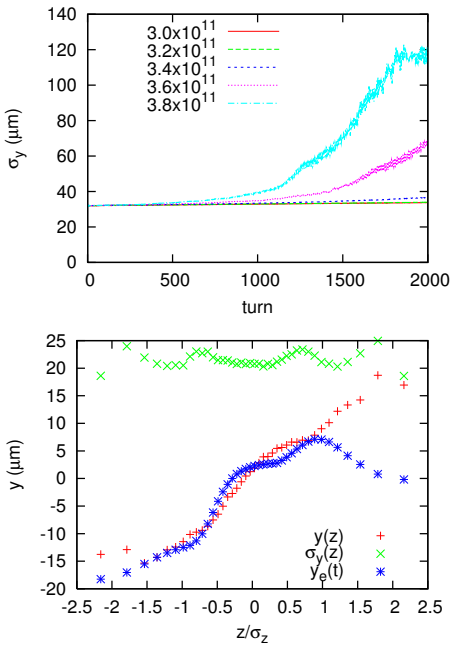

Figure 1: Simulation of single bunch instability caused by electron cloud. Top plot shows evolution of vertical beam size, and bottom plot shows intra-bunch oscillation and electron motion.

condition by a coasting beam model determines the threshold of electron density as [5]

$$\rho_{e,th} = \frac{2\gamma\nu_s\omega_c\sigma_z/c}{\sqrt{3}KQr_e\langle\beta_y\rangle L}. \quad (4)$$

The quality factor Q is characterized by nonlinear interaction of beam and electron cloud. The nonlinear component of Q is evaluated by a numerical simulation as $Q_{nl} \approx 5-15$ depending on the cloud size and beam shape (flat or round). One typical value is $Q_{nl} = 6.3$ for interaction of flat beam and electron cloud with the size of $10\sigma_x \times 10\sigma_y$ [4]. Wake force with longer range than the bunch length does not contribute to the instability. Therefore Q is effectively described by

$$Q = min(Q_{nl}, \omega_c\sigma_z/c). \quad (5)$$

The frequency of the wake force is 25% larger than ω_c for the typical case. It is between ω_c and ω_e.

K characterizes enhancement of wake force strength depending on how much electrons contribute the instability. For KEKB, $K \approx 3$ for $\omega_c\sigma_z/c \approx 3$ [4]. We assume $K \approx \omega_c\sigma_z/c$, because the number of electrons, which contribute to the instability, is proportional to $\omega_c\sigma_z/c$.

For low emittance ring, $\omega_c\sigma_z/c$ is large. It is larger than $Q_{nl} = 6.3$ for $N_p > 1.3\times10^{10}$ for Phase-I, II parameters. The effective Q is constant $Q = Q_{nl} = 6.3$. The threshold is constant assuming $K = \omega_e\sigma_z/c$,

$$\rho_{e,th} = \frac{2\gamma\nu_s}{\sqrt{3}Q_{nl}r_e\langle\beta_y\rangle L} = 2.8\times10^{11}\ \mathrm{m}^{-3}, \quad (6)$$

where the averaged vertical beta function $\langle\beta_y\rangle = 12$ m.

VERTICAL EMITTANCE GROWTH DUE TO ELECTRON CLOUD INSTABILITY

In the early stage of Phase-I commissioning, a vertical emittance growth had been observed. The reason why the instability arose was that 5% of the LER ring were not coated by TiN [6]. The 5% area is near joint of chambers with bellows. Fortunately the appearance of the emittance growth was a good opportunity for studying threshold behavior of the single bunch electron cloud instability.

We studied the emittance growth for bunch train with various filling. Figure 2 shows the vertical beam size, measured by the X-ray monitor [7], as a function of beam current for several bunch filling, 2, 3, 4, 6 bucket spacing, where the total number of bunches is 600. Thresholds of the beam

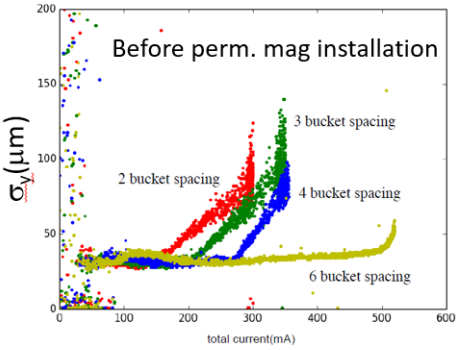

Figure 2: Beam size as a function of beam current.

current for each bunch spacing are obtained from the figure. They are 160, 200, 260 and 500 mA for 2, 3, 4 and 6 bucket spacing, respectively. Corresponding bunch populations are 1.6, 2.0, 2.7 and 5.2×10^{10}, respectively.

Simulations using the beam parameters were executed to evaluate threshold of electron density. Figure 3 presents simulation results for $N_p = 1.6, 2.0, 2.7$ and 5.2×10^{10}. The threshold density is summarized in Figure 4. The threshold density is weakly dependent on the bunch population, $\rho_{e,th} = 3 \sim 4\times10^{11}\ \mathrm{m}^{-3}$.

The electron density at area with/without the TiN coating is measured using a test chamber [8]. Figure 5 presents the measured electron density as a function of beam current in various bunch filling at the test chamber. Top and bottom plots show electron density without and with TiN coating, respectively. The density without TiN coating is very high and rapidly increases as function of the beam current. The density at the region without TiN coating is 2.0, 3.2, 4.3 and $8.1\times10^{12}\ \mathrm{m}^{-3}$ at the threshold for fillings with 2, 3, 4, 6 bucket spacing, respectively, in Figure 2. The corresponding densities with TiN coating are 2.5, 2.0, 2.0 and $2.3\times10^{11}\ \mathrm{m}^{-3}$.

The joint area, 5% of the ring, was not coated by TiN. The contribution to whole ring is 1.0, 1.6, 2.2 and $4.1\times10^{11}\ \mathrm{m}^{-3}$. In the early stage of Phase-I commissioning, no cure had been applied in the joint area. On average, beam expe-

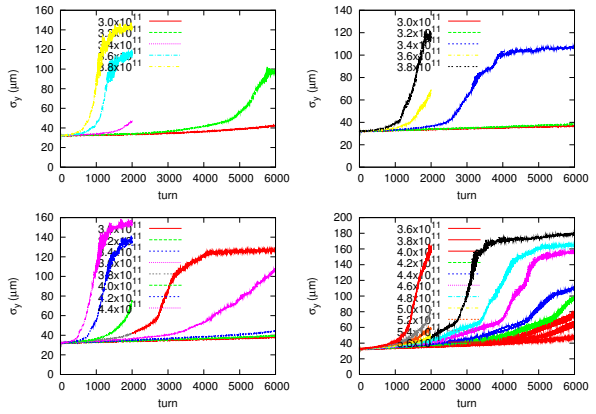

Figure 3: Vertical emittance growth in simulation PEHTS. Top left, top right, bottom left and bottom right are evolution of the vertical beam size for $N_p = 1.6, 2.0, 2.7$ and 5.2×10^{10}, respectively.

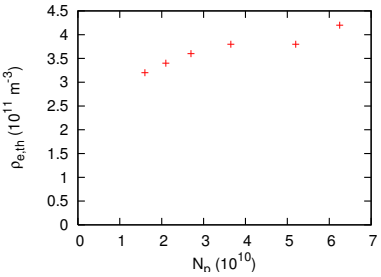

Figure 4: Instability threshold of electron density determined by the simulation using PEHTS.

riences electron cloud with the density 3.4, 3.5, 4.1 and 6.3×10^{11} m^{-3} at the threshold of each filling.

The emittance growth was suppressed by installation of permanent magnets at the joint area, The magnets produce an axial field ($B_z \sim 100$ G) at the chamber surface effectively. Figure 6 shows measured beam size after installation of the magnets. Threshold beam currents of the emittance growth were 200 and 330mA for 2 and 3 bucket spacing , respectively, and higher than 600 mA for 4 or more bucket spacing. The threshold electron density is evaluated from the bottom (with TiN coating) of Figure 5, if electrons at the joint area are perfectly cleared.

Table 2 summarizes the threshold current and electron density at the threshold for each bunch spacing. Top 4 lines and bottom 3 lines correspond to conditions before and after the permanent magnet installation, respectively.

The threshold of 2 bucket spacing ($N_p = 2.1 \times 10^{10}$) is serious for the design bunch population (9×10^{10}). For Phase-II commissioning, further permanent magnets were attached at most (86%) of the beam chambers in drift space. The emittance growth has not been observed in Phase-II until $N_p = 4.5 \times 10^{10}$ with 2 bucket spacing.

Table 2: Summary of threshold of the vertical emittance growth.

$N_{p,th}$ 10^{10}	$\omega_e\sigma_z/c$	$\rho_{e,sim}$	$\rho_{e,mon}$ 10^{11} m^{-3}	spacing	$I_{p,th}$ mA
1.6	6.8	3.2	3.4	2	160
2.1	7.8	3.2	3.5	3	200
2.7	8.9	3.6	4.1	4	260
5.2	12.3	3.8	6.3	6	500
2.1	7.8	3.2	3.0	2	200
3.65	10.3	3.8	3.0	3	350
6.25	13.5	4.2	2.0	4	>600

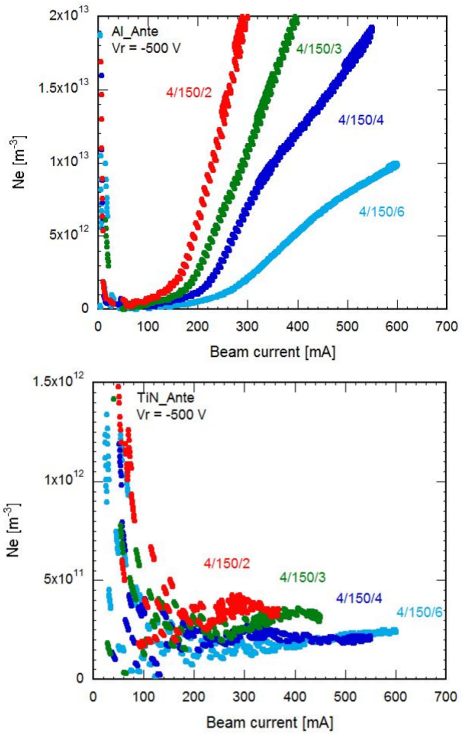

Figure 5: Measured electron density at a test chamber. Top and bottom are density without and with TiN coating, respectively, as a function of beam current in various bunch filling.

TUNE SHIFT DUE TO ELECTRON CLOUD

Electron cloud causes a positive tune shift due to the attractive force between beam and electron cloud. The tune shift depends on the electron density and distribution. For a static round charge distribution, tune shift is expressed by

$$\Delta\nu_x = \Delta\nu_y = \frac{\rho_e r_e \langle\beta_{x,y}\rangle}{2\gamma} C \qquad (7)$$

For flat distribution along x,

$$\Delta\nu_x = 0, \qquad \Delta\nu_y = \frac{\rho_e r_e \langle\beta_{x,y}\rangle}{\gamma} C \qquad (8)$$

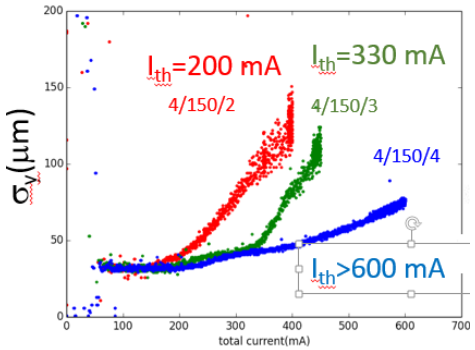

Figure 6: Measured vertical beam size after permanent magnet installation.

Transverse tune was measured along the bunch train for 3 bucket spacing filling. Figure 7 shows horizontal (top) and vertical (bottom) tune of bunches at 0, 150,300 and 450-th bucket.

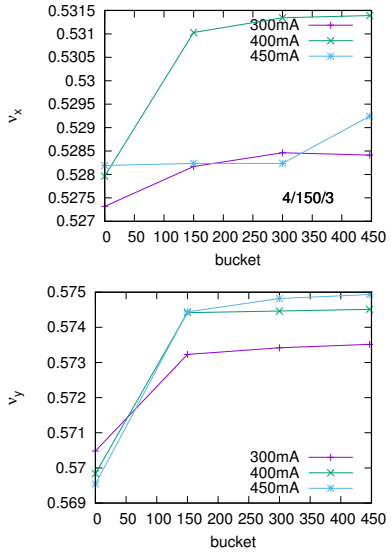

Figure 7: Tune shift along bunch train for 3 spacing filling.

The horizontal tune shift depends on the beam current (I): i.e., $\nu_x = 0.003$ for $I = 400$ mA and $\nu_x = 0.001$ for $I = 300$ and 450 mA. The horizontal tune shift seems to be ambiguous. The vertical tune shift is $\nu_y = 0.005$. The electron density is estimated to be $\rho_e = 4 \times 10^{11}$ m^{-3}, if only the vertical tune shift is considered. For $\nu_x + \nu_y = 0.006 - 0.008$, the density is $\rho_e = 5 - 6 \times 10^{11}$ m^{-3}. The density is in good agreement with that directly measured in the test chamber with/without TiN coating.

CONCLUSION

Beam commissioning of Phase-I was performed in February to June in 2016 without interaction region and Phase-II commissioning was performed in March to July 2018 after installation of IR magnets and the BELLE-II detector. Study of electron cloud effects was one of the highest priority issue in the commissioning. Fast head-tail instability due to electron cloud was observed at the predicted density, and was suppressed by axial field in uncoated bellows area of TiN as expected. Electron density were measured during the commissioning progress. The measured tune shift was consistent with the threshold value of the electron density. Further permanent magnets, which produce axial field, were attached at most (86%) of the beam chambers for Phase-II commissioning. The emittance growth has not been observed in Phase-II until $N_p = 4.5 \times 10^{10}$ with 2 bucket spacing.

ACKNOWLEDGEMENT

The authors thank SuperKEKB team for the commissioning and operation and help for machine experiments.

REFERENCES

[1] K. Ohmi, F. Zimmermann, Phys. Rev. Lett. 85, 3821 (2000).

[2] K. Ohmi, Phys. Rev. Lett. 75, 1526 (1995).

[3] Y. Suetsugu et al., Phys. Rev. AB 19, 121001 (2016).

[4] K. Ohmi, F. Zimmermann, E. Perevedentsev, Phys. Rev. E 65, 016502 (2001).

[5] A. W. Chao, *Physics of Collective Beam Instabilities in High Energy Accelerators*, Wiley-Interscience Publication, New York, 1993), and references therein.

[6] Y. Suetsugu et al., proceedings of IPAC17, WEPIK008 (2017).

[7] E. Mulyani, J. Flanagan, H. Ikeda, H. Fukuma, M. Tobiyama, proceedings of IPAC18, THPML074.

[8] Y. Suetsugu et al., in this proceedings (2018).